Catalysis Letters Vol. 105, Nos. 3–4, December 2005 (© 2005)
DOI: 10.1007/s10562-005-8700-y

Changes in Ba phases in BaO/Al_2O_3 upon thermal aging and H_2O treatment

Do Heui Kim*, Ya-Huei Chin, Ja Hun Kwak, János Szanyi, and Charles H.F. Peden*

Pacific Northwest National Laboratory, Institute for Interfacial Catalysis, 902 Battelle Boulevard MSIN K8-93, P.O. Box 999, Richland, WA 99352, USA

Received 23 July 2005; accepted 12 September 2005

The effects of thermal aging and H_2O treatment on the physicochemical properties of BaO/Al_2O_3 (the NO_x storage component in the lean NO_x trap systems) were investigated by means of X-ray diffraction (XRD), BET, TEM/EDX and NO_2 TPD. Thermal aging at 1000 °C for 10 h converted dispersed $BaO/BaCO_3$ on Al_2O_3 into low surface area crystalline $BaAl_2O_4$. TEM/EDX and XRD analysis showed that H_2O treatment at room temperature facilitated a dissolution/reprecipitation process, resulting in the formation of a highly crystalline $BaCO_3$ phase segregated from the Al_2O_3 support. Crystalline $BaCO_3$ was formed from conversion of both $BaAl_2O_4$ and a dispersed $BaO/BaCO_3$ phase, initially present on the Al_2O_3 support material after calcinations at 1000 and 500 °C, respectively. Such a phase change proceeded rapidly for dispersed $BaO/BaCO_3/Al_2O_3$ samples calcined at relatively low temperatures with large $BaCO_3$ crystallites observed in XRD within 10 min after contacting the sample with water. Significantly, we also find that the change in barium phase occurs even at room temperature in an ambient atmosphere by contact of the sample with moisture in the air, although the rate is relatively slow. These phenomena imply that special care to prevent the water contact must be taken during catalyst synthesis/storage, and during realistic operation of $Pt/BaO/Al_2O_3$ NO_x trap catalysts since both processes involve potential exposure of the material to CO_2 and liquid and/or vapor H_2O. Based on the results, a model that describes the behavior of Ba-containing species upon thermal aging and H_2O treatment is proposed.

KEY WORDS: BaO/Al_2O_3; $BaAl_2O_4$; lean NO_x trap; NO_2 TPD; NO_x storage; nitric oxide.

1. Introduction

During recent years, lean NO_x traps (LNTs) are considered as one of the most promising solutions for gasoline lean burn and diesel engine exhaust emission control in order to meet stringent requirements on emission levels being implemented in the immediate future [1]. This technology, introduced in 1994 by researchers at Toyota [2], is based on the switching of the engine operating conditions between lean and rich cycles. Typical LNT catalysts consist of 1–2 wt% of precious metal (Pt and Rh) and 10–20 wt% of a storage material (Ba or K) dispersed on an Al_2O_3 support. During the lean cycle, excess NO_x is oxidized over Pt and stored as nitrate on the storage material. When the engine is subsequently switched to the oxygen-deficient stage, i.e. the rich cycle, stored nitrates are released and/or reduced to N_2. It has been recognized that deactivation on LNTs is related to poisoning of Ba storage sites by sulfur oxides in the exhaust, and by high temperature regeneration treatments that result in undesirable changes in material properties of the LNTs. Under typical operating conditions, low levels of SO_2 in the exhaust cumulatively deposit onto the barium NO_x storage sites, gradually converting these sites into $BaSO_4$ [3]. Because formation of $BaSO_4$ is thermodynamically favored over both $BaCO_3$ and $Ba(NO_3)_2$, this process is irreversible at typical LNT operating conditions [4] causing severe activity losses in the NO_x storage-reduction function. In order to retransform $BaSO_4$ into $BaCO_3$ and/or BaO, a high temperature treatment of the NO_x storage material is required to regenerate the storage catalyst. However, during this high temperature regeneration, i.e. above 800 °C, sintering of Pt metal and the formation of low surface area $BaAl_2O_4$ take place. Such material changes not only give rise to poor interaction between Pt and the Ba storage sites, but also may lead to a decrease of total available sites for NO_x storage. Both of these processes are thought to contribute to LNT deactivation [1,5]. Therefore, a current challenge in LNT catalyst research is to develop a stable storage material that can withstand both SO_2 poisoning and high temperature treatment.

Recently, a group at Ford Motor Company [6] reported X-ray diffraction (XRD) studies showing that Ba^{2+} ions in a $BaAl_2O_4$ phase were leached out to form crystalline $BaCO_3$ upon contact with H_2O, and proposed that this was due to an interaction with carbonic acid dissolved in liquid H_2O. The process of barium phase change can be understood by analogy with the degradation of $CaAl_2O_4$, a well established reaction in the cement industry. The degradation of $CaAl_2O_4$, one of the main components in cement, into $CaCO_3$ is called

* To whom correspondence should be addressed.
E-mail: do.kim@pnl.gov; chuck.peden@pnl.gov

1011-372X/05/1200–0259/0 © 2005 Springer Science+Business Media, Inc.

"carbonation" [7,8], which has a negative effect on the cement stability. As the Ford group observed for $BaAl_2O_4$, the carbonation process for cement is initiated by exposure of $CaAl_2O_4$ to moisture in the air. Considering the importance of the barium species as the storage material in LNTs, a more detailed investigation of the physicochemical changes of the barium species arising from H_2O and thermal aging, and the understanding of the carbonation process are warranted.

In order to further understand the effects of thermal aging and H_2O treatment on the physicochemical properties of BaO/Al_2O_3 LNT materials, we performed NO_2 temperature programmed desorption (TPD), transmission electron microscopy coupled with energy dispersive X-ray spectroscopy (TEM/EDX), BET surface area measurements, and powder XRD with samples treated under various conditions. To exclude the effects of different crystalline Pt particle size caused by thermal treatment, a Pt-free BaO/Al_2O_3 material was selected for this initial study. The goal of this work was to understand the behavior of barium containing species when applying thermal and/or H_2O treatments, thereby providing guidance for the preparation and operation of LNT catalysts containing more durable barium species. In this study, we have shown that, in addition to the formation of $BaCO_3$ from $BaAl_2O_4$, highly dispersed barium carbonate species are transformed to a segregated crystalline $BaCO_3$ phase upon exposure to H_2O; this latter result has not been previously reported and may have important implications for both catalyst preparation and actual LNT operation.

2. Experimental

2.1. Catalyst preparation

About 20 wt% BaO/Al_2O_3 catalysts were prepared by incipient wetness impregnation using barium acetate (99%, Aldrich ACS reagent) as a precursor on a commercial γ-alumina support (Engelhard AL-3945). Prior to impregnation, the as-received alumina was first calcined by heating in a muffle furnace under ambient air at 5 °C/min to 500 °C and held isothermally at 500 °C for 3 h. An aqueous solution containing barium acetate was prepared and subsequently added to the calcined alumina by incipient wetness at room temperature. To achieve a 20 wt% Ba loading, two sequential impregnations were required due to the low solubility of Ba acetate in water. Between impregnations, the sample was dried again at 110 °C for 8 h. After final impregnation, the catalyst precursor material was dried at 110 °C overnight, and subsequently calcined in air following the 500 °C calcination procedure described above. For comparison purposes, barium nitrate (99%, Aldrich ACS reagent) was used as a precursor instead of barium acetate and calcined under air flowing to exclude the formation of carbonate species arising from the oxidation of the acetate precursor.

Various additional thermal treatments were performed on the as calcined sample in a muffle furnace under ambient conditions. H_2O treatment was carried out at room temperature with H_2O added to the thermally treated BaO/Al_2O_3 samples with an amount exceeding the incipient wetness point until the sample appeared in a paste form and completely immersed in liquid water, at a ratio of approximately 1 cc water per g of BaO/Al_2O_3. The H_2O treated samples were allowed to dry at room temperature overnight, then calcined at 500 °C, following the temperature programmed procedure described above. To investigate the effect of CO_2 in the ambient air during the drying process, we treated the samples with H_2O in a N_2 purged glove bag, followed by drying them under N_2.

2.2. Catalyst characterization

Transmission electron microscopy (TEM) imaging was conducted on a JEOL 2010 high-resolution analytical electron microscope operating at 200 kV with a LaB_6 filament. The TEM instrument includes an energy dispersive X-ray (EDX) spectrometer as well. Powdered samples were dispersed in ethanol then mounted on copper grids containing a Formvar/carbon support film.

The XRD data was collected on a Philips X'Pert MPD (Model PW3040/00) instrument with a vertical 2θ goniometer (190 mm radius). The X-ray source was a long fine-focus and sealed ceramic X-ray tube (Cu anode) operated at 40 kV and 50 mA (2000 W). The optical train consisted of programmable divergence, anti-scatter, and receiving slits, incident and diffracted beam soller slits, a curved graphite diffracted beam monochromator, and a Xe-filled proportional counter detector. The diffraction data were analyzed using Jade 5 (Materials Data Inc., Livermore, CA) and the Powder Diffraction File database (International Centre for Diffraction Data, Newtown Square, PA).

A Micromeritic Tristar Gas Adsorption analyzer was used for BET surface area measurements. Samples were degassed in flowing N_2 at 200 °C prior to these measurements.

TPD following NO_2 adsorption at room temperature was performed in a fixed bed microcatalytic quartz reactor. In order to avoid unintended ambient formation of a $BaCO_3$ crystalline phase (as described in the Results and Discussion section below), TPD experiments were performed over all samples within one week after the above described 500 °C calcinations prior to TPD. About 100 mg of sample was pre-treated *in situ* under He (UHP grade) flow at 200 °C for 1 h. After cooling down in a He flow to room temperature, a 0.5% NO_2/He (99.999% Purity, Matheson) gas mixture was passed over the catalyst until saturation. All gas flows were metered by mass flow controllers (Brooks Co.).

After saturation, the catalyst was purged with He for 2 h to remove the physisobed NO_x species, and then the temperature was raised to 800 °C at a constant rate of 8 °C/min under He flow (50 cm^3/min). The evolution of both NO and NO_2 during the TPD experiment were monitored with a chemiluminescence NO_x analyzer (42C, Thermo Environmental).

3. Results and discussion

3.1. Effect of thermal aging

Figure 1 shows XRD patterns of 20 wt% BaO/Al_2O_3 samples after calcination in air at different temperatures. The XRD of a BaO/Al_2O_3 sample calcined at 500 °C showed diffraction patterns with broad peaks ascribed to crystalline orthorhombic $BaCO_3$ and gamma (γ) Al_2O_3 phases. Heat treatment in air decomposes the Ba acetate precursor to crystalline $BaCO_3$, as previously described by Nova and co-workers [4,9]. Additional heat treatment at an elevated temperature of 900 °C for 2 h appears to decompose the crystalline $BaCO_3$, as evidenced from the disappearance of multiplet peaks characteristic of crystalline orthorhombic $BaCO_3$ ($2\theta = 23.8$–24.8, 33.7–34.5, and 41.9–44.9; PDF 45-1471). However, no other barium related phase was detected as a result of $BaCO_3$ decomposition. According to temperature-programmed synchrotron XRD during the decomposition of $Ba(NO_3)_2/Al_2O_3$ under a He flow [10], heating this type of sample above 600 °C in oxygen results in the formation of nano crystalline BaO particles ~5 nm in size. Therefore, it can be presumed that BaO/Al_2O_3, after calcinations at 900 °C, contains nano crystalline BaO and/or $BaCO_3$ which is not detected by XRD using typical laboratory instrumentation. Calcination at 1000 °C for 10 h resulted in the formation of a new phase, with diffraction peaks ($2\theta = 19.60$, 28.20 and 34.30), ascribed to $BaAl_2O_4$ in the spinel structure (PDF 17-0306). Such a transformation is thermodynamically favored as a result of a solid state reaction between BaO/$BaCO_3$ and Al_2O_3. Not surprisingly, the BET surface area of these samples decreased with increasing heat treatment temperature, as shown in Table 1. The decrease in the surface area was attributed to the formation of low surface area $BaAl_2O_4$, and to the increasing crystallinity of the γ-Al_2O_3 support as also indicated in the XRD patterns.

TPD profiles for NO_2 and NO obtained after room temperature NO_2 adsorption on 20 wt% BaO/Al_2O_3 calcined at different temperatures are shown in figure 2. There are two main desorption peaks, corresponding to NO_2 and NO desorption at ~420 °C and at ~530 °C, respectively. These two desorption peaks have been proposed to originate from the decomposition of a monolayer and bulk barium nitrate phases, respectively. These assignments were made on the basis of the results of our recent TPD, FTIR, and ^{15}N NMR studies of NO_2 adsorption on BaO/Al_2O_3 samples [11]. In the NMR experiments, we have observed two different nitrate species, formed from a reaction between NO_2 and the supported Ba phase, at chemical shifts of 337 and 340.5 ppm (relative to $^{15}NH_4Cl$). The intensity ratios of these two peaks varied with BaO coverage, and clearly related to the intensity ratios of the NO_2 and NO desorption features in the NO_2 TPD spectra.

As shown in figure 2, the amount of NO desorbed from a 20 wt% BaO/Al_2O_3 sample, calculated by integrating the area under the higher temperature NO

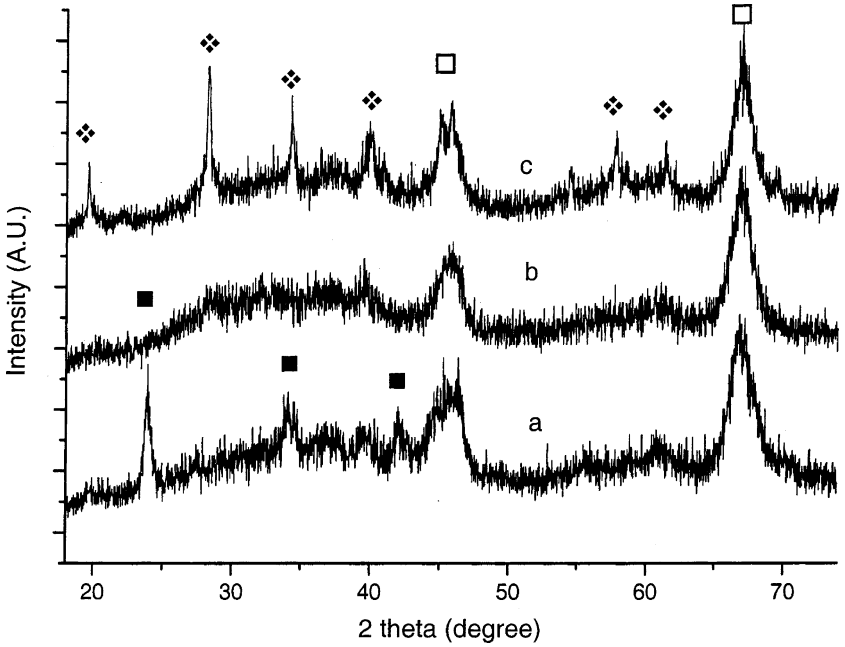

Figure 1. XRD patterns of 20 wt% BaO/Al_2O_3 samples calcined at 500 °C (a), 900 °C (b) and 1000 ° (c) (■ $BaCO_3$, □: γ-Al_2O_3, ❖: $BaAl_2O_4$)

Table 1
BET surface area calcined and water treated Bao/Al_2O_3 samples (m^2/g)

Sample	Initial	H_2O treated
Al_2O_3	218.4	
Bao/Al_2O_3 calcined at 500 °C for 3 h	156.8	171.0
Bao/Al_2O_3 calcined at 900 °C for 2 h	125.3	187.0
Bao/Al_2O_3 calcined at 1000 °C for 10 h	104.1	157.9

phase, formed after aging the BaO/Al_2O_3 at high temperatures (≥750 °C). The transformation was proposed to be similar to that observed for the leaching of Ca from $CaAl_2O_4$ phases in cement (so-called "carbonation" [7,8]), a result of "weathering". More significantly, we have discovered that performing the same H_2O treatment on a BaO/Al_2O_3 sample calcined at more moderate temperatures of ~500 °C, where there is no

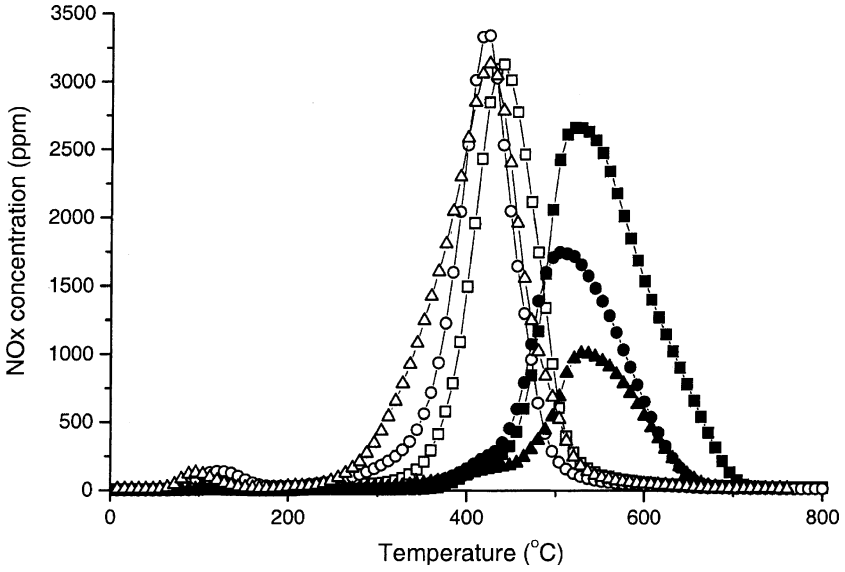

Figure 2. NO_2 TPD spectra in He over 20 wt% BaO/Al_2O_3 samples calcined at 500 °C (■, square), 900 °C (●, circle) and 1000 °C (▲, triangle). Open and solid symmbols indicate NO_2 and NO, respectively.

desorption profile, decreased significantly with increasing calcination temperature. On the other hand, the total amount of NO_2 desorbed at ~420 °C remained essentially constant. XRD analysis, as shown in figure 1, clearly indicates a change in the state of the Ba-containing phase after high temperature treatments. Interestingly, these samples exhibited similar NO_2 evolution profiles during NO_2 TPD, regardless of phase of Ba present in the samples. Based on these assignments, it is suggested that as thermal aging proceeds, the $BaAl_2O_4$ phase forms at the expense of a bulk Ba species, as indicated by the suppression of NO desorption in the TPD profiles with increasing thermal aging temperatures.

3.2. *Effect of H_2O treatment*

The formation of highly crystalline $BaCO_3$ is evidenced after treatment of a thermally aged 20 wt% BaO/Al_2O_3 sample with liquid H_2O at room temperature, as shown in XRD patterns displayed in figure 3b and 3c. Contacting a thermally aged BaO/Al_2O_3 with liquid H_2O at room temperature initiates the transformation of Ba containing phases into a highly crystalline $BaCO_3$ phase. Such a transformation was first reported by Graham, *et al.* [6]. at Ford research, and the authors attributed it to the leaching of Ba from a $BaAl_2O_4$ evidence for $BaAl_2O_4$ formation, also results in the formation of large $BaCO_3$ crystallites (figure 3a). Thus, the growth of $BaCO_3$ phases cannot be explained in all samples by "carbonation" because, for the 500 °C calcined sample, no $BaAl_2O_4$ is present before water treatment. Rather in the later case, $BaCO_3$ crystallite size growth can be accounted for by a dissolution/reprecipitation process without the need to leach Ba from a crystalline alumina-containing phase. Indeed, formation of crystalline $BaCO_3$ was evidenced on all BaO/Al_2O_3 samples after water treatment, regardless of the initial state of Ba. Moreover, it should be pointed out that the crystallite size of the $BaCO_3$ phase in BaO/Al_2O_3 calcined at 500 °C is much larger than those of higher temperature thermally aged samples (figure 3b and 3c), as evidenced by the narrower diffraction peaks in the XRD patterns of the former sample. This result will be discussed later.

Transmission electron microscopy coupled with energy dispersive X-ray microanalysis (TEM/EDX) was used to further probe morphological changes in the water treated samples. TEM images of the BaO/Al_2O_3 sample calcined at 500 °C (result not shown here) display a morphology similar to that of the γ-Al_2O_3 support. This is not surprising, since it is well established that BaO is dispersed on the γ-Al_2O_3 surfaces and

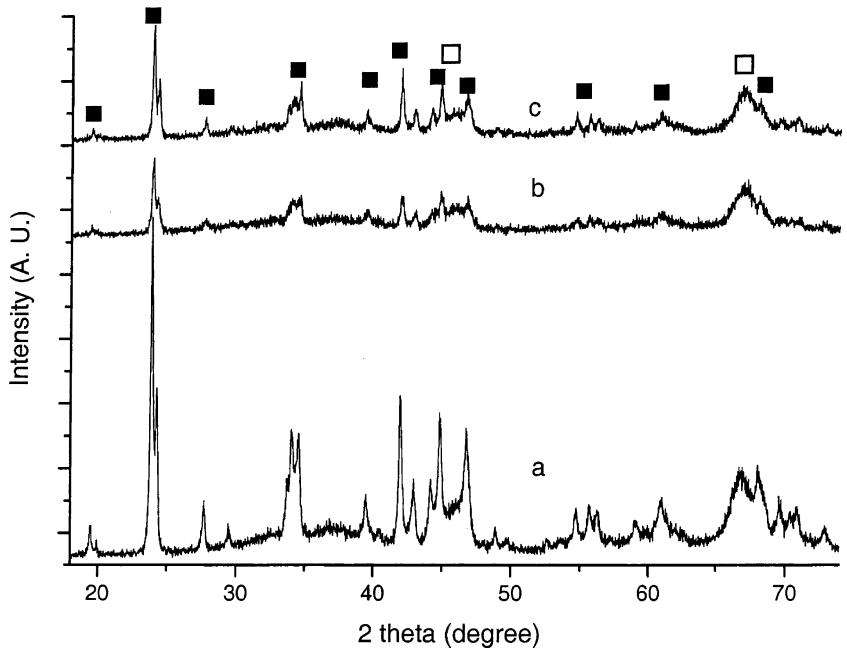

Figure 3. XRD patterns of H_2O-treared 20 wt% BaO/Al_2O_3 samples; H_2O treatment was performed after calcining BaO/Al_2O_3 at 500 °C (a), 900 °C (b) and 1000 °C (c) (■ $BaCO_3$, □: γ-Al_2O_3).

therefore not detectable under typical TEM imaging modes due to insufficient contrast [10]. Similarly, TEM images of BaO/Al_2O_3, obtained after thermal treatments at 900 and 1000 °C show no significant structural changes even though XRD and BET data indicate considerable morphological changes including the formation of $BaAl_2O_4$. EDX microanalysis over a number of areas in the TEM images shows uniform Ba and Al distributions for all three of these samples.

Significant changes in the TEM images and EDX microanalysis occurred after treating the BaO/Al_2O_3 samples in H_2O. Figure 4 shows two micrographs taken after H_2O treatment of BaO/Al_2O_3 samples that have been pre-calcined at 500 °C (a) and 1000 °C (b). Both samples, when compared with their non-water-treated counterparts, show distinct textural changes caused by the H_2O treatment. After H_2O treatment two distinct phases can be seen in the TEM images: one resembling that of the non-treated samples (essentially the morphology of the Al_2O_3 support), and the other showing large crystals formed by the H_2O treatment. These two phases were separated and co-existed in a physical mixture-like state. EDX microanalysis (figure 4) was performed on selected areas marked in the TEM micrographs in order to compare the chemical composition of the two distinct phases. For all of these analyses, X-ray counts contributed by Al and Ba species were detected, albeit with dramatically different levels. In particular, EDX spectra from regions of the TEM image resembling the γ-Al_2O_3 support itself display high X-ray counts for Al with a small, often negligible contribution from Ba. In contrast, EDX analyses from the newly visible crystalline phases show intense X-ray contributions from Ba. As noted above, XRD data show the formation of large $BaCO_3$ crystallites from these same samples. Thus, the combined results of TEM/EDX and XRD studies allow us to conclude that the interaction of the samples with H_2O leads to the formation of large $BaCO_3$ crystals segregated from the Al_2O_3 support.

The segregation of the $BaCO_3$ phases from the BaO/Al_2O_3 samples was also evidenced by NO_2 TPD performed on the H_2O treated samples, as presented in figure 5. Notable changes in higher temperature NO desorption profiles were observed after water treatment of the samples. Comparing with the TPD of samples without water treatment in figure 2, the NO desorption temperature remained the same at approximately 530 °C, however, the desorption peaks became significantly sharper. We believe that this high temperature NO desorption with a "sharp" profile can be ascribed to desorption arising from bulk decomposition of nitrates formed by NO_2 adsorption on highly ordered, large $BaCO_3$ crystallites. Centi, *et al.* [12] claimed that the NO_x storage process on BaO proceeds through the formation of bulk barium nitrate, governed by bulk diffusion. This process is slow due to expansion of the crystalline unit cell associated with conversion of BaO to $Ba(NO_3)_2$. NO desorption from these presumably poorly ordered Ba nitrate species would be expected to result in a broad desorption profile.

On the other hand, NO_2 adsorption features are complex. In particular, it is difficult to distinguish the NO_2 desorption from monolayer BaO and the Al_2O_3

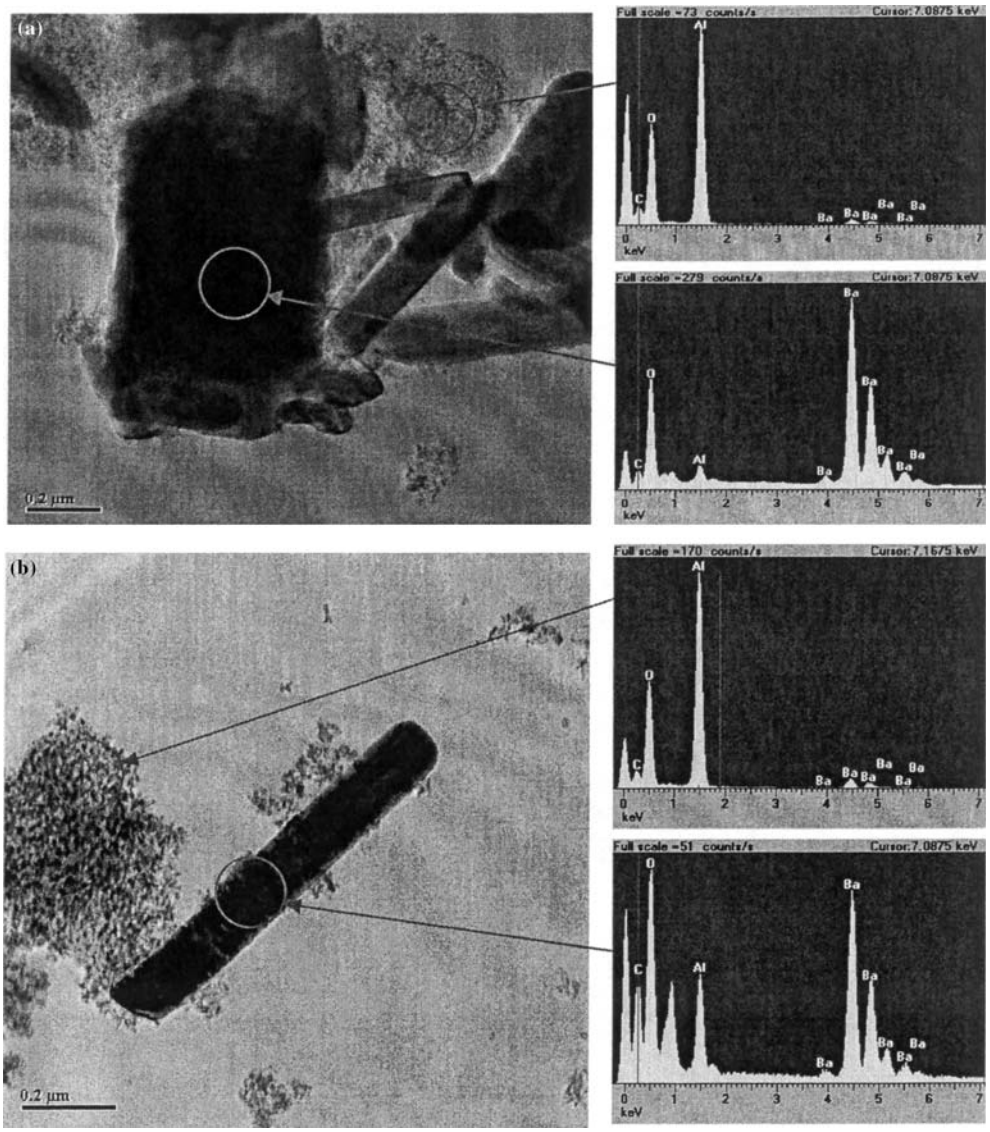

Figure 4. TEM images and EDX spectra of selected areas of H_2O-treated BaO/Al_2O_3 samples. BaO/Al_2O_3 was pre-calcined at 500 °C (a), and 1000 °C (b), before the H_2O-treatment.

support, because the main NO_2 desorption peaks from these two sources both occur around 400 °C in TPD [11]. It seems likely that, following contact of the sample with H_2O promoting the segregation of $BaCO_3$ from the Al_2O_3 support, 'uncovers' at least some Al_2O_3 adsorption sites for NO_2 adsorption.

3.3. Effect of H_2O treatment conditions

In order to understand the dissolution/reprecipitation process of the barium-containing phases for calcined BaO/Al_2O_3 samples in more detail, we investigated the effect of water treatment on the structural changes under various conditions with XRD. The first parameter varied was temperature at which the sample was treated with CO_2 and H_2O. We treated a freshly 500 °C-calcined, 20 wt % BaO/Al_2O_3 sample with a flow of 10% H_2O vapor and 10% CO_2 balanced with helium at 150 °C overnight. The XRD pattern following treatment at 150 °C (not shown) was virtually identical to the one obtained from a non-H_2O treated sample. Furthermore, the BET surface area was not changed at all by this treatment. These observations suggest that dissolution of barium phases, described above, takes place only in the presence of liquid H_2O, most likely under conditions where the solubility of CO_2 in H_2O was high; e.g., at room temperature.

In the dissolution/reprecipitation process, the carbonate ion can be derived from several carbon sources; i.e., residual carbon species and/or barium carbonate species initially present on the catalyst surface from the catalyst precursor and/or calcining conditions [13], gaseous (atmospheric) CO_2 dissolved into liquid water during the drying process, and carbonate ions already

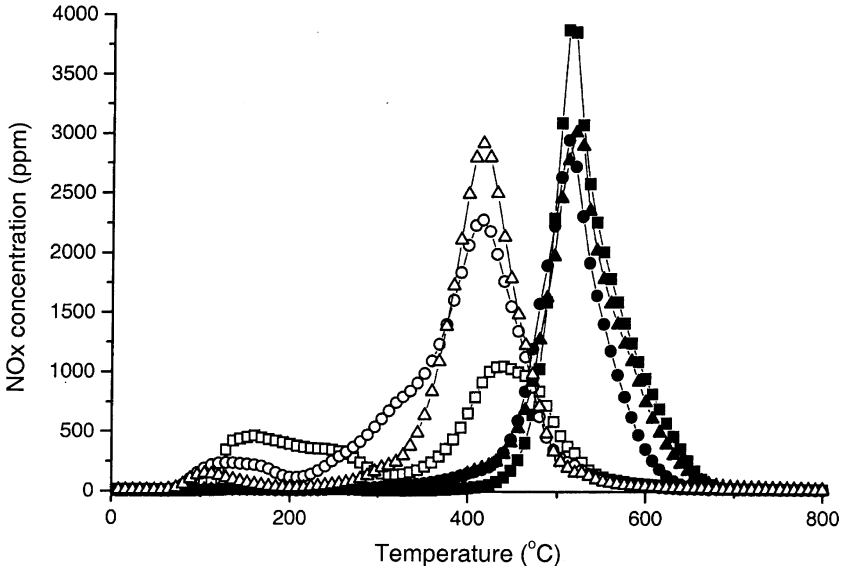

Figure 5. NO_2 TPD spectra in He over H_2O-treated 20 wt% BaO/Al_2O_3 samples. BaO/Al_2O_3 was calcined at 500 °C (■, square), 900 °C (●, circle) and 1000 °C (▲, triangle) prior to water treatment. Open and solid symbols indicate NO_2 and NO, respectively.

present in H_2O. To investigate the source of carbon, we prepared a BaO/Al_2O_3 sample that is free of residual carbon using barium nitrate instead of barium acetate as the precursor (denoted as BaO/Al_2O_3-N) and treated the sample with water. The BaO/Al_2O_3-N was calcined at 500 °C under flowing dry air (zero grade) and the water treatment was performed inside a N_2-purged glove bag to minimize contamination of the sample by gas phase CO_2 adsorbing on the surface. Water-treated BaO/Al_2O_3-N samples were dried at room temperature under either N_2 flow in a glove bag or in ambient air. Figure 6 shows the XRD patterns of various BaO/Al_2O_3 samples dried under different conditions after H_2O treatment. Between the two XRD patterns of BaO/Al_2O_3-N, the air dried sample (figure 6b) contained significantly more crystalline $BaCO_3$ phase than the N_2-dried one (figure 6a), suggesting that gaseous CO_2 plays a critical role in the dissolution/precipitation process by maintaining a sufficiently high equilibrated concentration of dissolved CO_2 in the aqueous solution contacting the sample during drying. Compared with BaO/Al_2O_3 (figure 6c) prepared from an acetate precursor, the $BaCO_3$ phase on the air dried BaO/Al_2O_3-N sample (figure 6b) appears to be less crystalline. That the former contains more carbonate (as $BaCO_3$) and likely additional residual carbon species than the latter before treatment with water implies that the pre-existing barium carbonate and/or residual carbon species are a significant "supplier" of carbonate ions to the process of growing the $BaCO_3$ crystalline phase, in addition to CO_2 in the ambient air.

The growth of $BaCO_3$ during drying of a water-treated BaO/Al_2O_3 sample was followed with XRD as shown in figure 7. After taking the XRD pattern of the 500 °C-calcined BaO/Al_2O_3 sample on the glass XRD holder (figure 7a), D.I. water was applied to the sample on the holder, until it appeared wet, just above the incipient wetness level. XRD scans were then initiated immediately (7b), and 4 h (7c) and 24 h (7d) later while the sample continuously dried on the XRD sample holder. The inset in figure 7 highlights the growth of the $BaCO_3$ phase by expanding the region around the $BaCO_3$ XRD peak at ~24° 2θ. While an entire XRD scan took approximately one hour to complete for the conditions used here, the region near 24° 2θ was scanned within 10 min of initiating the scan. Thus as shown in figure 7, the crystallite size of $BaCO_3$ was large already after drying at room temperature for as little as 10 min, and continued to slowly increase in size up to 4 h after the liquid water was removed by evaporation. Further drying time had no additional effect on the $BaCO_3$ crystalline size. Recall that water treatment of the $BaAl_2O_4$ phase in high-temperature thermally aged BaO/Al_2O_3 samples gave rise to a less crystalline $BaCO_3$ phase than highly dispersed BaO/Al_2O_3 samples calcined at lower temperatures (figure 3). This may be related to the relative ease of dissolving Ba ions during water contact and, thus, their relatively higher concentrations during water evaporation and coincident reprecipitation of $BaCO_3$ for the samples calcined at lower temperature.

In fact, we obtained evidence that this process can occur without contacting the samples with liquid water. Figure 8 presents XRD patterns of the BaO/Al_2O_3 samples, which were left in ambient air for one day (figure 8a) and for 6 months (figure 8b) after initial 500 °C-calcinations, clearly showing the formation of crystalline $BaCO_3$ at ambient conditions over a prolonged period of time. We note here, in contrast to the characteristic doublet peak for a highly crystalline

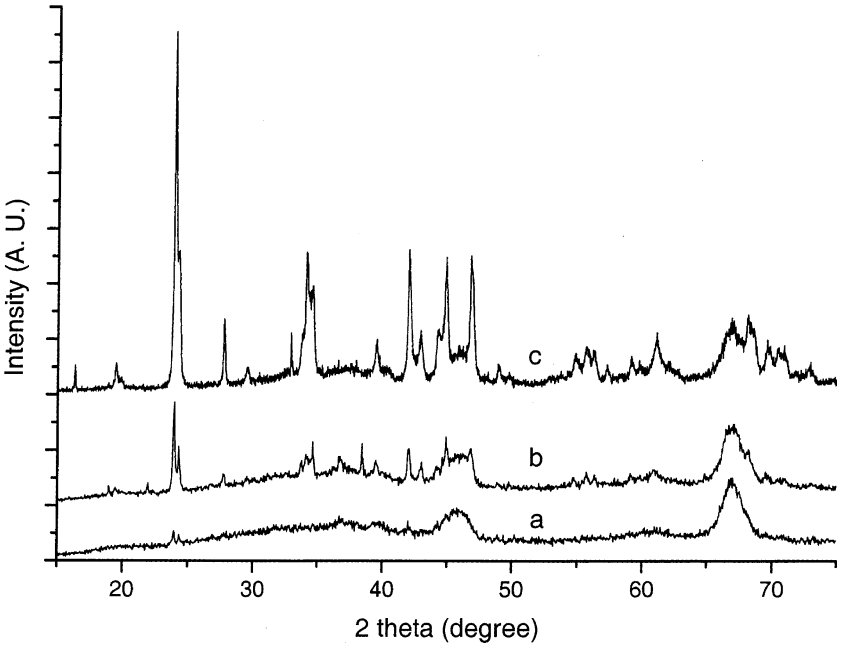

Figure 6. XRD patterns of various 20 wt% BaO/Al_2O_3 samples dried at different conditions after H_2O treatment (1 cc/g). After adding the water to BaO/Al_2O_3-N, it was dried at room temperature; (a) under N_2 flow and (b) under ambient air. (c)The same condition as (b) over BaO/Al_2O_3.

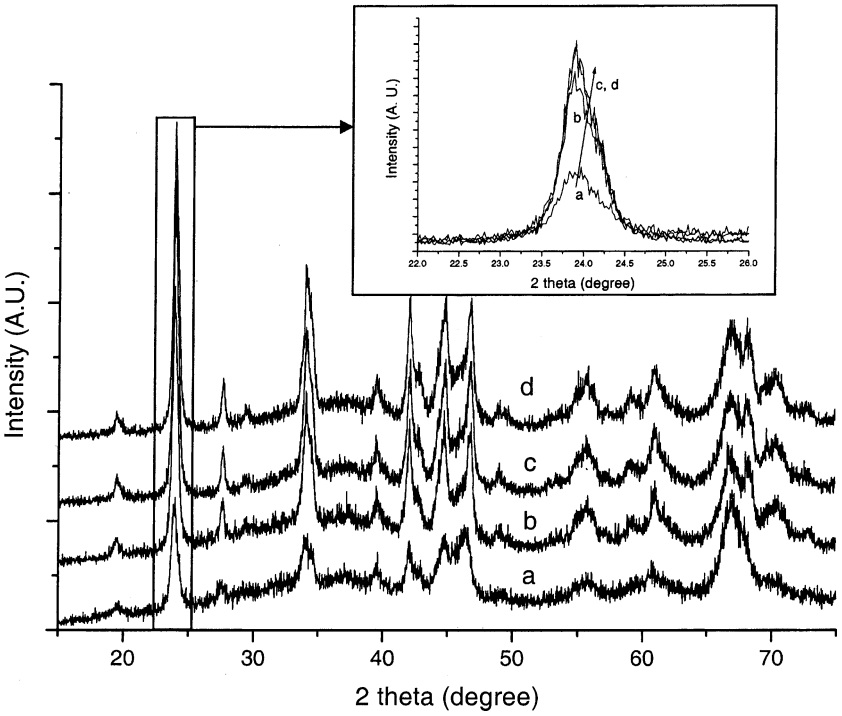

Figure 7. XRD patterns of various 20 wt% BaO/Al_2O_3 samples at different conditions; (a) as-calcined; after drying at room temperature in the ambient air (b) for 0.5 h, (c) for 4 h, and (d) for 24 h prior to H_2O treatment.

$BaCO_3$ phase at $\sim 24°$ 2θ (figure 6), that a somewhat broader peak in figure 8b is observed indicating that the $BaCO_3$ phase obtained after ambient air treatment is less well-ordered. Recalcination at 500 °C (figure 8c) results in little, if any, change with $BaCO_3$ still evident. We believe that a similar dissolution/reprecipitation of barium takes place by contacting the sample with the moisture and CO_2 in ambient air,

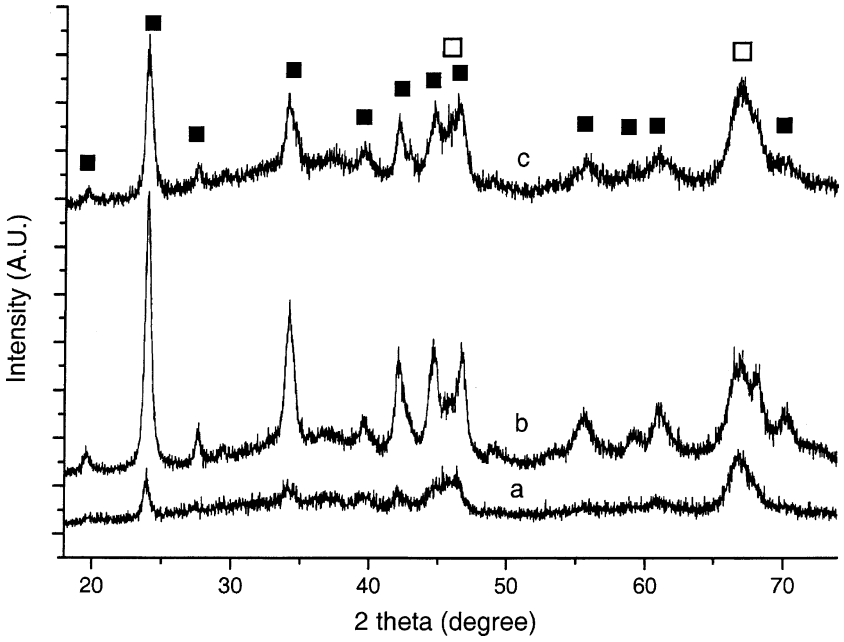

Figure 8. XRD patterns of various 20 wt% BaO/Al_2O_3 calcined at 500 °C (a) taken after one day, and (b) after 6 months from the initial calcinations. Pattern (c) was taken after 1 day following recalcination of BaO/Al_2O_3 from pattern (b) (■: $BaCO_3$, □: γ-Al_2O_3).

although the rate is significantly slower than when liquid water is used.

3.4. Proposed mechanism

Based on the results, a model that describes the behavior of BaO/Al_2O_3 with respect to thermal aging and water treatment is illustrated in figure 9. After calcination at 500 °C, Ba is most likely present in the form of small BaO and/or $BaCO_3$ crystallites highly dispersed on the alumina support. After aging the sample at high temperatures, a $BaAl_2O_4$ phase with the spinel structure is formed by a solid state reaction between the Ba species and the Al_2O_3 support, resulting in the depletion of the bulk barium phase ($BaCO_3$ and/or BaO). Irrespective of the initial barium phase (highly dispersed BaO or $BaCO_3$, or $BaAl_2O_4$), liquid H_2O treatment at room temperature facilitates dissolution and reprecipitation of Ba species, to produce large crystallites of $BaCO_3$ segregated from the Al_2O_3 support. The resulting material can be described as a physical mixture of $BaCO_3$ crystallites and Al_2O_3 support material. In this process, temperature was an important factor probably because liquid water contacted the surface and because the solubility of CO_2 in H_2O was higher at lower temperature. It has been proposed [6] that the presence of liquid water containing dissolved CO_2, particularly inside the BaO/Al_2O_3 pores, is responsible for the leaching of Ba from the BaO/Al_2O_3 material. We believe that this is the first study to report the segregation of $BaCO_3$ crystallites from Al_2O_3 support material as a result of contacting with water, as evidenced by the TEM/EDS results discussed above. Notably we showed that the Ba phase dissolution/reprecipitation processes not only takes place over samples containing $BaAl_2O_4$ phases, but also on fresh BaO/Al_2O_3 samples calcined at lower temperatures.

These findings may have significant implications for the current NO_x-trap system, since H_2O condensation is

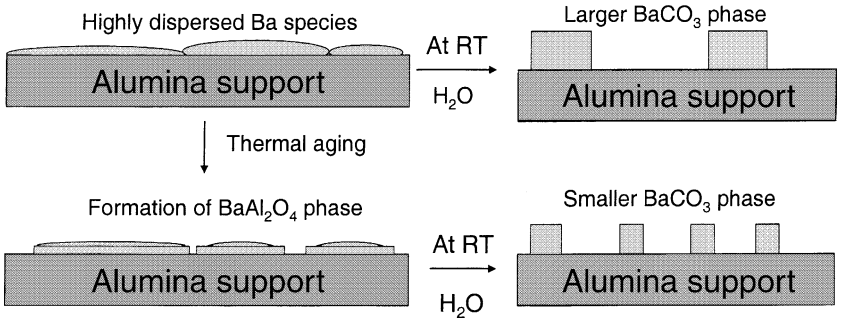

Figure 9. Proposed carbonation mechanism of barium species on Bao/Al_2O_3.

known to occur in exhaust systems during start-up and shut-down of the engine [6]. Additionally under normal engine operation conditions, the exhaust gas mixture contains at least 10% H_2O and 10% CO_2. Therefore, a real NO_x trap catalyst is continuously in contact with CO_2 gas and water vapor, and potentially with liquid water at low temperature where dissolution/reprecipitation processes can occur. These effects may also need to be considered when optimizing the synthesis of NO_x trap catalysts. Conventional incipient wetness impregnation methods are commonly used to sequentially add Pt and barium to the alumina support material [14,15]. If barium is added first, the resultant BaO/Al_2O_3 material will therefore be in contact with liquid water during the Pt deposition step from an aqueous solution, perhaps leading to the undesirable formation of segregated Ba species.

4. Conclusion

Thermal aging of a 20 wt% BaO/Al_2O_3 sample at 1000 °C for 10 h resulted in formation of a crystalline $BaAl_2O_4$ phase by reaction between dispersed $BaO/BaCO_3$ and Al_2O_3 at the interface, leading to a decrease of bulk NO_x adsorption sites. It was shown that H_2O treatment at room temperature facilitates a dissolution/reprecipitation process, resulting in the formation of crystalline $BaCO_3$ segregated from the Al_2O_3 support. The process converted both $BaAl_2O_4$ and dispersed $BaO/BaCO_3$ on alumina into crystalline $BaCO_3$, as shown in TEM, XRD, NO_2 TPD, and BET measurements. Such a phase change proceeded rapidly for dispersed $BaO/BaCO_3/Al_2O_3$ samples calcined at relatively low temperatures with large $BaCO_3$ crystallites observed in XRD within 10 min after contacting the sample with water. Significantly, we also find that the change in barium phase occurs even at room temperature in an ambient atmosphere by contact of the sample with moisture in the air, although the rate is relatively slow. These results imply that special care must be taken during catalyst synthesis, and during the storage of $Pt/BaO/Al_2O_3$ NO_x trap catalysts. It may also have consequences for the practical operation of NO_x trap catalysts due to the unavoidable contact of H_2O, CO_2 and the catalyst in these processes. Based on the results presented here, a model was proposed to explain the behavior of the Ba species after thermal aging and/or water treatment of BaO/Al_2O_3 NO_x trap materials.

Acknowledgments

We acknowledge the financial support from the U.S. Department of Energy (DOE), Office of FreedomCar and Vehicle Technologies. We also acknowledge the CRADA partners (Cummins Inc. and Johnson Matthey Catalysts) for allowing us to publish these results. The experiments were performed in the Environmental Molecular Sciences Laboratory (EMSL) at Pacific Northwest National Laboratory (PNNL). The EMSL is a national scientific user facility and supported by the US DOE's Office of Biological and Environmental Research. PNNL is a multi-program national laboratory operated for the U.S. Department of Energy by Battelle Memorial Institute under contract number DE-AC06–76RLO 1830.

References

[1] W.S. Epling, L.E. Campbell, A. Yezeretz, N.W. Currier and J.E. Parks II, Catal. Rev. Sci. Eng. 46 (2004) 163.
[2] S. Matsumoto, Catal. Today 29 (1996) 43.
[3] P. Engström, A. Amberntsson, M. Skoglundh, E. Fridell and G. Smedler, Appl. Catal. B 22 (1999) L241.
[4] L. Lietti, P. Forzatti, I. Nova and E. Tronconi, J. Catal. 204 (2001) 175.
[5] B.-H. Jang, T.-H. Yeon, H.-S. Han, Y.-K. Park and J.-E. Yie, Catal. Lett. 77 (2001) 21.
[6] G.W. Graham, H.-W. Jen, J.R. Theis and R.W. McCabe, Catal. Lett. 93 (2004) 3.
[7] S. Goñi, M.T. Goztañaga and A. Guerrero, J. Mater. Res. 17 (2002) 1834.
[8] H.F.W. Taylor, in: *Cement Chemistry*, edited by H.F.W. Taylor (Academic Press, London, United Kingdom, 1992), Ch. 10, pp. 333.
[9] F. Prinetto, G. Ghiotti, I. Nova, L. Lietti, E. Tronconi and P. Forzatti, J. Phys. Chem. B 105 (2001) 12732.
[10] J. Szanyi, J.H. Kwak, J. Hanson, C. Wang, T. Szailer and C.H.F. Peden, J. Phys. Chem. B 109 (2005) 7339.
[11] J. Szanyi, J.H. Kwak, D.H. Kim, S.H. Burton and C.H.F. Peden, J. Phys. Chem. B 109 (2005) 27.
[12] G. Centi, G.E. Arena and S. Perathoner, J. Catal. 216 (2003) 443.
[13] M. Piacentini, M. Maciejewski and A. Baiker, Appl. Catal. B 59 (2005) 137.
[14] L. Olsson and E. Fridell, J. Catal. 210 (2002) 340.
[15] G.E. Arena, A. Bianchini, G. Centi and F. Vazzana, Top. Catal. 16/17 (2001) 157.